Journal of Oral Biology and Craniofacial Research 16 (2026) 66–72

Contents lists available at ScienceDirect

Journal of Oral Biology and Craniofacial Research

journal homepage: www.elsevier.com/locate/jobcr

Biogenic synthesis of copper oxide nanoparticles using *Alpinia calcarata* extract promotes osteoblasts differentiation: An *In vitro* study

Rathika Ravi [a], Deepavalli Arumuganainar [b,*]

[a] *Saveetha Medical College, Saveetha Institute of Medical and Technical Sciences, Saveetha University, Chennai, Tamil Nadu, India*
[b] *Department of Periodontics, Saveetha Dental College and Hospital, Saveetha Institute of Medical and Technical Sciences, Saveetha University, Chennai, Tamil Nadu, India*

ARTICLE INFO

Keywords:
Copper oxide nanoparticles
Alpinia calcarata
Green synthesis
Osteogenesis
Mesenchymal stem cells
Bone tissue engineering

ABSTRACT

Background: Copper-based biomaterials are increasingly investigated for bone tissue engineering due to their osteogenic and angiogenic properties. Green synthesis using plant extracts offers an eco-friendly route for producing biocompatible nanoparticles. This study aimed to synthesize copper oxide nanoparticles (CuO NPs) using *Alpinia calcarata* leaf extract and evaluate their cytocompatibility and osteogenic potential in vitro.

Methods: CuO NPs were synthesized by reacting copper nitrate trihydrate with A. calcarata leaf extract under alkaline conditions, followed by calcination. The nanoparticles were characterized using SEM, TEM, XRD, and FTIR to confirm morphology, crystallinity, and functional group interactions. C3H10T1/2 murine mesenchymal stem cells were used to assess cytocompatibility (MTT assay, FDA staining), osteogenic differentiation (Alizarin Red S staining and quantification), and gene expression (qRT-PCR for Runx2, Col-I, and ALP).

Results: SEM and TEM revealed aggregated, spherical nanoparticles of <100 nm, while XRD confirmed crystalline monoclinic CuO and FTIR indicated phytochemical capping. MTT and FDA assays showed CuO NPs were cytocompatible up to 50 μg/mL, with dose-dependent cytotoxicity observed at higher concentrations. Under osteogenic conditions, cells treated with 50 μg/mL CuO NPs displayed significantly enhanced mineral deposition compared to controls. Gene expression analysis demonstrated upregulation of Runx2, Col-I, and ALP, confirming promotion of osteogenic differentiation.

Conclusion: Biogenically synthesized CuO NPs using A. calcarata extract are structurally pure, biocompatible at defined concentrations, and capable of enhancing osteoblast differentiation by stimulating matrix mineralization and osteogenic gene expression. These findings position A. calcarata–mediated CuO NPs as sustainable, multifunctional nanomaterials with promising applications in bone tissue engineering.

1. Introduction

Critical-sized bone defects remain difficult to treat because autografts/allografts carry risks of donor-site morbidity, limited availability, and inconsistent biological activity, motivating bioactive materials that can orchestrate both osteogenesis and angiogenesis in situ. Among trace elements, copper has emerged as particularly promising: in bone and cartilage tissue engineering, copper-containing biomaterials have shown pro-osteogenic, pro-angiogenic and antibacterial effects, attributable in part to controlled Cu^{2+} release from scaffolds.[1] Systematic and mechanistic work further indicates that ionic copper can tune early neovascularization—an essential prerequisite for stable bone regeneration—by stimulating endothelial responses and coupling them to osteoblast activity.[2,3] Recent preclinical studies using copper-modified bioactive glasses and composites report improved cytocompatibility, osteogenic differentiation, and angiogenic signaling compared with copper-free controls, with benefits reproduced in rodent defect models.[4] In parallel, green (biogenic) nanotechnology has gained traction as a sustainable alternative to chemical routes for copper oxide nanoparticle (CuO NPs) fabrication. Plant extracts—rich in reductive and capping phytochemicals (flavonoids, phenolics, terpenoids)—can nucleate and stabilize CuO under mild conditions, typically yielding monoclinic CuO confirmed by XRD and phytochemical signatures by FTIR.[5–7] Multiple plant systems (e.g., Aerva javanica, Opuntia

* Corresponding author. Department of Periodontics, Saveetha Dental College and Hospitals, Saveetha Institute of Medical and Technical Sciences, Saveetha University, Chennai, Tamil Nadu, India.
E-mail addresses: rathikaravi2002@gmail.com (R. Ravi), deepavallia.sdc@saveetha.com (D. Arumuganainar).

https://doi.org/10.1016/j.jobcr.2025.11.007
Received 30 August 2025; Accepted 8 November 2025
Available online 14 November 2025

ficus-indica, Aegle marmelos) have produced phase-pure CuO NPs with tunable size and surface chemistry that exhibit favorable bioactivity profiles in vitro.[5,8,9] Comprehensive reviews from 2020 to 2024 emphasize that such biogenic CuO often displays improved colloidal stability and reduced synthesis-related toxicity relative to conventional routes, while retaining the desirable reactivity of copper oxides.[6,7] Within this space, the Zingiberaceae genus Alpinia is compelling as a green reagent source. *Alpinia calcarata* (AC) contains abundant oxygenated monoterpenes and polyphenols (e.g., 1,8-cineole, α-terpineol, camphor) alongside tannins and flavonoids, which act as natural reductants/capping ligands and also impart antioxidant and anti-inflammatory activities.[10,11] Detailed pharmacognostic and essential-oil studies on AC (2015–2024) catalog these constituents and demonstrate bioactivities that could be advantageous both during nanoparticle formation (reduction/capping) and at the cell–material interface (e.g., quenching excess ROS).[10,11] Despite this phytochemical richness and the success of other plant systems, AC-mediated CuO synthesis and its implications for bone remain underexplored—representing a tractable opportunity for biogenic, bone-active CuO NPs. From a biological standpoint, osteogenic differentiation of mesenchymal stem cells (MSCs) is governed by a canonical program. RUNX2 functions as the master transcription factor for osteoblast lineage commitment; its sustained activity drives expression of bone matrix genes and progression from osteoprogenitors to pre-osteoblasts and mature osteoblasts.[12] Type I collagen (Col-I) provides the principal organic scaffold of bone and organizes the mineral phase during matrix maturation.[13] Alkaline phosphatase (ALP) is a hallmark early osteogenic enzyme that promotes mineral deposition by generating inorganic phosphate and degrading inhibitory pyrophosphate, thereby enabling hydroxyapatite nucleation within the collagenous matrix.[14] Coordinated upregulation of RUNX2, Col-I, and ALP is thus a recognized molecular signature of osteogenesis in vitro and in vivo. Integrating these strands suggests a twofold rationale. First, biogenic CuO NPs produced with AC extract could merge (i) the ionic bioactivity of copper—known to enhance osteogenesis/angiogenesis—with (ii) plant-derived surface moieties that stabilize colloids and may modulate cell responses. Second, copper can participate in osteo-angiogenic crosstalk via signaling axes such as canonical Wnt and HIF-1α, potentially amplifying pro-osteogenic transcription (RUNX2) and pro-angiogenic factors (e.g., VEGF) when released from a nanomaterial matrix.[3] Indeed, recent studies show Cu-modified glasses and composites upregulate osteogenic genes and angiogenic readouts in MSCs and improve defect repair in vivo.[1,4,15,16] Accordingly, the present study reports the biogenic synthesis of CuO nanoparticles using *Alpinia calcarata* leaf extract, physicochemical validation (SEM, TEM, XRD, FTIR), and in-vitro evaluation of cytocompatibility and osteogenic efficacy in the C3H10T1/2 MSC's. We hypothesized that AC-derived CuO NPs would be phase-pure and sub-100-nm, and under osteogenic conditions would increase RUNX2, ALP, and Col-I expression and enhance mineralized matrix formation—thereby defining a sustainable, bioactive nanomaterial platform for bone regeneration.

2. Methodology

2.1. Preparation of Alpinia calcarata leaf extract

Fresh leaves of *Alpinia calcarata* (40 g) were first washed thoroughly under running tap water, followed by rinsing with distilled water to eliminate dust and surface impurities. The cleaned leaves were shade-dried and finely chopped into small fragments before being ground into a coarse paste. The plant material was then extracted by boiling with 200 mL of distilled water for 60 min at 50–70 °C using a Soxhlet extraction unit (500 mL round-bottom flask). This procedure ensures efficient extraction of bioactive polyphenolic compounds, including flavonoids and non-flavonoids, which are known to function as reducing and capping agents in nanoparticle synthesis. Once the extraction was completed, the mixture was cooled to ambient temperature, passed through a strainer to remove coarse debris, and subsequently filtered using Whatman No. 1 filter paper. The clear filtrate obtained was collected and stored in airtight containers at 4 °C until further use in nanoparticle synthesis.

2.2. Green synthesis of CuO nanoparticles

For nanoparticle preparation, 100 mL of 0.1 M copper nitrate trihydrate [$Cu(NO_3)_2{\cdot}3H_2O$] solution was prepared in distilled water in a 500 mL beaker. To this, 20 mL of the previously prepared *Alpinia calcarata* leaf extract was slowly introduced with continuous stirring at 70–80 °C using a magnetic stirrer. To adjust the alkalinity, freshly prepared sodium hydroxide (0.2 mmol) was added dropwise until the solution pH reached 10. The reaction mixture was maintained under vigorous stirring for 4 h, during which a dark precipitate of copper oxide nanoparticles (CuO NPs) gradually formed. The precipitate was allowed to settle, collected, and washed sequentially 4–5 times with distilled water and ethanol to remove unreacted precursors and impurities. The purified material was then dried on a clean watch glass and subsequently transferred to a crucible for calcination. The sample was heated in a muffle furnace at 420 °C for 3 h, which facilitated crystallization and uniform particle formation. The calcined CuO NPs were then cooled and stored for subsequent applications.

2.3. Physico-chemical characterization

To confirm the morphology, structure, and functional groups of the synthesized copper oxide nanoparticles (CuO NPs), different characterization techniques were employed, including SEM, TEM, XRD, and FTIR. The surface morphology and particle aggregation of the synthesized CuO NPs were studied using a Scanning Electron Microscope (JEOL JSM-6390LV, Japan) operated at an accelerating voltage of 15 kV. Prior to imaging, the powdered sample was mounted on a double-sided carbon adhesive tape fixed on an aluminum stub and sputter-coated with a thin gold layer using a Quorum SC7620 sputter coater to enhance conductivity and avoid charging. Micrographs were recorded at varying magnifications to examine nanoparticle shape and distribution pattern. The fine morphology and crystallinity of the nanoparticles were analyzed using Transmission Electron Microscopy (JEOL JEM-2100, Japan) operated at 200 kV. For sample preparation, approximately 2 mg of CuO NPs were ultrasonically dispersed in 5 mL of ethanol for 15 min. A small drop of the suspension was placed on a carbon-coated copper grid (300 mesh) and air-dried before imaging. The crystalline structure and phase purity of CuO NPs were determined using an X-ray diffractometer (PANalytical X'Pert PRO, Netherlands) with Cu-Kα radiation ($\lambda = 1.5406$ Å) as the X-ray source. The powdered sample was analyzed over a 2θ range of 10°–80°, with a step size of 0.02° and a scanning rate of 2°/min under operating conditions of 40 kV and 30 mA. The diffraction peaks obtained were compared with the standard JCPDS database for CuO. Functional groups responsible for the stabilization and capping of CuO NPs by *Alpinia calcarata* extract were examined using FTIR spectroscopy (Shimadzu IRTracer-100, Japan). The dried CuO nanoparticle sample was finely mixed with spectroscopic grade potassium bromide (KBr) and compressed into a thin pellet. Spectral data were collected in the mid-infrared range of 4000–400 cm^{-1}.

2.4. Cell culture and maintenance

The murine mesenchymal stem cell line C3H10T1/2 was purchased from NCCS, Pune, India and used for the cytotoxicity and osteogenic differentiation studies. Cells were cultured in Dulbecco's Modified Eagle Medium (DMEM, high glucose) supplemented with 10 % fetal bovine serum (FBS) and 1 % penicillin-streptomycin under standard conditions at 37 °C in a humidified atmosphere with 5 % CO_2. Cells were passaged at 70–80 % confluency using 0.25 % trypsin-EDTA and only passages 4–8 were used for experiments.

2.5. Cytotoxicity evaluation by MTT assay

The effect of CuO NPs on cell viability was assessed using the MTT colorimetric assay. Cells were seeded in 96-well plates at a density of 1 × 10^4 cells/well and incubated overnight to allow adherence. The culture medium was then replaced with fresh medium containing CuO NPs at concentrations of 1, 10, 25, 50, 100, and 200 μg/mL. After 24 h of exposure, 20 μL of MTT solution (5 mg/mL in PBS) was added to each well and incubated for 4 h at 37 °C. The resulting purple formazan crystals were dissolved in 200 μL of DMSO, and absorbance was measured at 570 nm using a microplate reader (BioTek Synergy H1, USA). Cell viability was expressed as a percentage relative to untreated control cells.

2.6. Cell viability and morphology by FDA staining

Fluorescein diacetate (FDA) staining was performed to visualize viable cells after nanoparticle exposure. Cells were seeded on sterile glass coverslips placed in 24-well plates and treated with CuO NPs (50 μg/mL) for 24 h. After treatment, cells were washed gently with phosphate-buffered saline (PBS) and incubated with 10 μg/mL FDA solution for 5 min in the dark. Excess dye was removed by PBS washing, and the stained cells were immediately observed under a fluorescence microscope (Nikon Eclipse Ti, Japan) with a FITC filter (excitation: 490 nm, emission: 520 nm). Live cells exhibited bright green fluorescence, confirming membrane integrity.

2.7. Osteogenic induction and Alizarin Red S staining

To evaluate osteogenic differentiation, C3H10T1/2 cells were cultured in osteogenic medium consisting of DMEM supplemented with 10 % FBS, 50 μg/mL ascorbic acid, 10 mM β-glycerophosphate, and 100 nM dexamethasone. Mineralized nodule formation was evaluated by Alizarin Red S (ARS) staining followed by quantification using sodium hydroxide. After treatment with CuO NPs (50 μg/mL) in osteogenic medium for 7 days, the cells were washed twice with PBS and fixed in 4 % paraformaldehyde for 15 min at room temperature. Following fixation, the monolayer was incubated with 2 % ARS solution (pH 4.2) for 20 min with gentle shaking, after which excess dye was removed and the wells were rinsed repeatedly with distilled water until the background was clear. Representative images of stained mineralized nodules were obtained under an inverted microscope. For quantification, the bound dye was eluted by adding 0.1 M NaOH (500 μL per well) and incubating the plate on a shaker for 15–30 min until complete solubilization. Aliquots of the eluted dye (200 μL) were transferred into a 96-well microplate, and absorbance was recorded at 570 nm using a microplate reader, with 0.1 M NaOH as blank. Quantitative results were expressed as mean absorbance values from triplicate wells.

2.8. Gene expression analysis by quantitative real-time PCR (qRT-PCR)

The expression of osteogenic marker genes Runx2, alkaline phosphatase (ALP), and collagen type I (Col-I) was assessed using quantitative real-time PCR. After 7 days of treatment with CuO NPs (50 μg/mL) in osteogenic medium, total RNA was extracted using the TRIzol reagent (Invitrogen, USA) according to the manufacturer's protocol. RNA concentration and purity were determined using a NanoDrop spectrophotometer (Thermo Fisher Scientific, USA). cDNA was synthesized from 1 μg of RNA using a RevertAid First Strand cDNA Synthesis Kit (Thermo Fisher, USA). qRT-PCR was carried out in a StepOnePlus Real-Time PCR System (Applied Biosystems, USA) using SYBR Green Master Mix (Thermo Fisher, USA). The relative expression levels of Runx2, ALP, and Col-I were normalized to GAPDH as the housekeeping gene, and fold changes were calculated using the $2^{-}\Delta\Delta Ct$ method.

2.9. Statistical analysis

All experiments were conducted in triplicate, and data are presented as mean ± standard deviation (SD). Statistical comparisons between treated groups and respective controls were performed using the Student's t-test. A p-value <0.05 was considered statistically significant. Analyses were carried out using GraphPad Prism version [insert version] (GraphPad Software, USA).

3. Results

3.1. Morphological analysis of CuO nanoparticles

The morphology of the synthesized copper oxide nanoparticles was examined using SEM and TEM analysis. SEM imaging (Fig. 1A) revealed that the nanoparticles were aggregated into densely packed clusters with a flower-like surface arrangement. The rough and porous nature of these assemblies suggests the availability of a large surface area, which is advantageous for potential biological and catalytic applications. TEM imaging provided further insight into the particle size and structural features (Fig. 1B). The nanoparticles were predominantly spherical in shape and displayed a uniform distribution with slight agglomeration. The size of individual particles was found to be in the sub-100 nm range, consistent with the expected nanoscale dimensions of CuO. Together, SEM and TEM observations confirmed the successful synthesis of well-defined copper oxide nanoparticles with distinct morphology suitable for downstream biological studies.

3.2. Physico-chemical characterization of CuO nanoparticles

The XRD analysis (Fig. 2A) reveals clearly defined diffraction peaks at ~35.6° and ~38.8°, which match well with reflections from the (−111), (002) and (111) planes characteristic of monoclinic copper oxide (CuO), as reported in related syntheses. Additional peaks at approximately 48.9°, 53.3°, 58.2°, and 61.6° correspond to other CuO crystal planes ((–202), (020), (202), and (−113), respectively). The absence of any peaks indicative of Cu_2O or other impurity phases supports the attainment of a pure CuO phase with a well-ordered monoclinic lattice. The obtained 2θ values corresponded well with the characteristic planes of CuO as documented in JCPDS card no. 00-041-0254. In the FTIR spectrum (Fig. 2B), a broad absorption centered near ~3426 cm^{-1} suggests the presence of O–H stretching, likely originating from surface-adsorbed water or residual hydroxyl groups. Peaks between 1600 and 1760 cm^{-1} may reflect C=O stretching or conjugated carbonyl functionalities, possibly from phytochemical capping agents. A notable absorption around 1367 cm^{-1} could correspond to N–O or C–N vibrations associated with nitrogenous groups. The strong, sharp bands in the fingerprint region, particularly around ~583 cm^{-1} and ~825 cm^{-1}, are consistent with Cu–O bending and stretching modes reported in similar CuO nanoparticles. Overall, the FTIR results confirm the presence of metal–oxygen bonds intrinsic to CuO nanoparticles as well as some functional groups from the leaf extract that likely contributed to nanoparticle stabilization.

3.3. CuO nanoparticles were found to be biocompatible

The cytotoxicity of CuO nanoparticles against C3H10T1/2 cells was assessed by MTT assay (Fig. 3A). At lower concentrations (1–50 μg/mL), no significant loss of cell viability was detected, with values comparable to the untreated control group. However, a clear dose-dependent decline was observed at higher concentrations, with approximately 70 % viability at 100 μg/mL and less than 50 % at 200 μg/mL. These results suggest that CuO NPs are biocompatible at lower concentrations but exert pronounced cytotoxic effects when the dose exceeds 100 μg/mL. To further confirm cell viability, FDA staining was performed (Fig. 3B). Untreated control cells (Panel I) displayed intense green fluorescence,

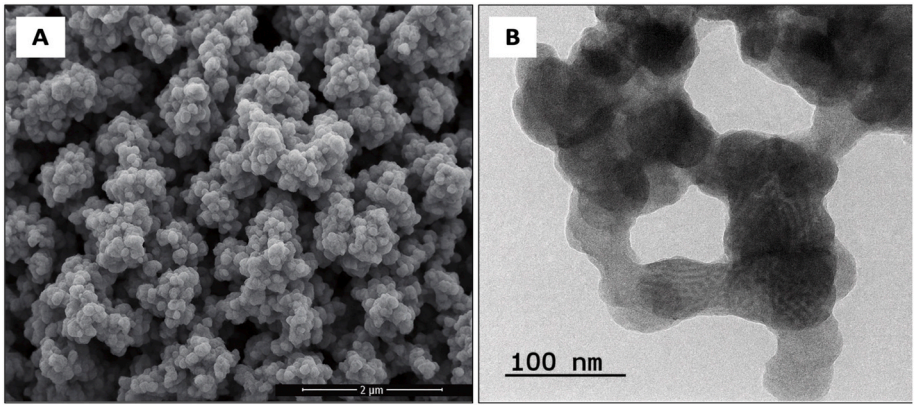

Fig. 1. Morphological characterization of CuO nanoparticles. (A) Scanning electron microscopy (SEM) image showing the surface morphology of synthesized CuO nanoparticles. The particles appear as irregular clusters with a aggregated structure. (B) Transmission electron microscopy (TEM) image displaying individual CuO nanoparticles at higher resolution. The average particle size was observed to be below 100 nm, confirming nanoscale dimensions.

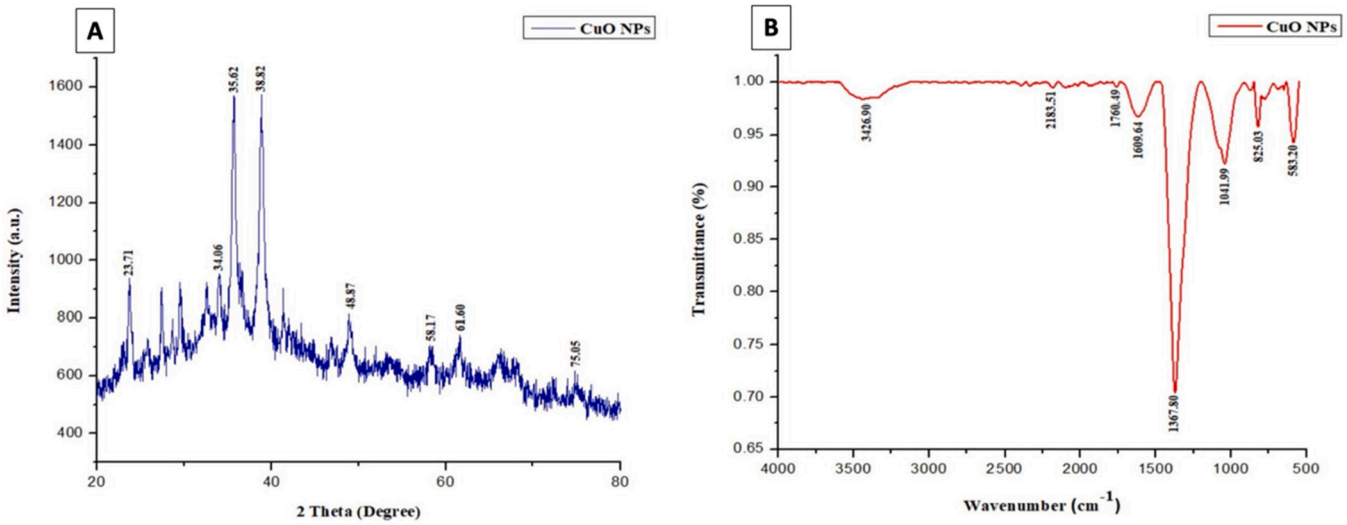

Fig. 2. Structural and functional group analysis of the synthesized CuO nanoparticles. (A) X-ray diffraction (XRD) pattern showing characteristic diffraction peaks and (B) Fourier-transform infrared (FTIR) spectrum of CuO NPs.

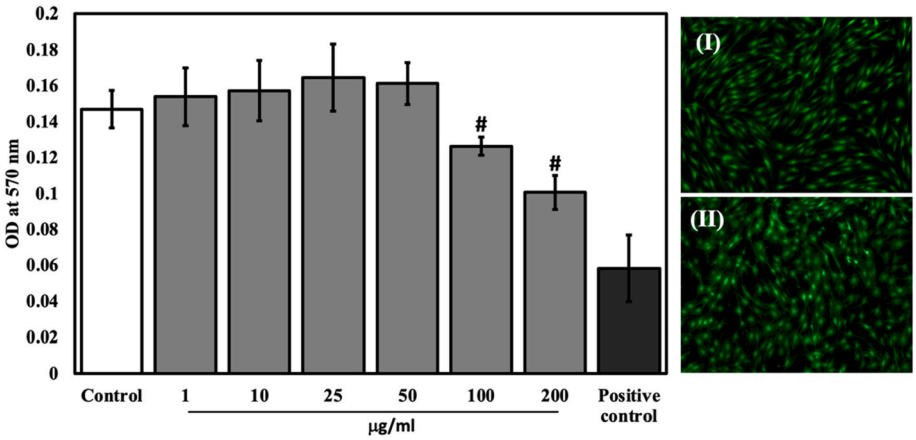

Fig. 3. Cytotoxicity and cell viability assessment of CuO nanoparticles on C3H10T1/2 cells. (A) Cell viability measured by MTT assay after 24 h exposure to different concentrations of CuO NPs (1–200 µg/mL). Data are expressed as mean ± SD from three independent experiments. A concentration-dependent reduction in viability was observed at higher doses. (B) Fluorescein diacetate (FDA) staining of C3H10T1/2 cells showing viable cells with intact membranes. Panel I: untreated control cells exhibiting uniform green fluorescence. Panel II: cells exposed to 50 µg/mL CuO NPs for 24 h showing slightly reduced fluorescence intensity, indicating moderate cytotoxicity.

indicative of healthy, metabolically active cells. In contrast, cells treated with 50 μg/mL CuO NPs (Panel II) exhibited slightly reduced fluorescence, consistent with moderate stress or partial loss of viability. Together, these findings demonstrate that CuO NPs maintain acceptable cytocompatibility at lower concentrations, supporting their suitability for subsequent osteogenic differentiation studies.

3.4. CuO nanoparticles promoted osteogenic differentiation under osteogenic conditions

The osteogenic potential of CuO nanoparticles was assessed by monitoring calcium-rich extracellular matrix deposition using Alizarin Red S staining (Fig. 4A). Cells grown in basal medium (control) exhibited minimal staining, indicating negligible mineralization. A moderate increase in red staining was observed in cells cultured in osteogenic medium (OM), reflecting induction of differentiation. Notably, the OM + CuO NP group displayed intense staining, with widespread mineral nodule formation, suggesting that CuO nanoparticles enhanced osteogenic activity.

Quantitative measurement of Alizarin Red dye elution confirmed these observations (Fig. 4B). The control group showed the lowest absorbance, while the OM group demonstrated a slight but not statistically significant increase. In contrast, cells treated with OM + CuO NPs exhibited a significant rise in mineralization, with absorbance values at 570 nm markedly higher than both control (*$p < 0.05$) and OM groups (#$p < 0.05$). These findings indicate that CuO nanoparticles promote osteogenic differentiation in C3H10T1/2 cells by enhancing matrix mineralization.

3.5. CuO nanoparticles enhanced the expression of osteoblast differentiation markers

The differentiation of mesenchymal stem cells (MSCs) into osteoblasts is orchestrated by the activation of several lineage-specific genes. Runt-related transcription factor 2 (Runx2) is regarded as the master regulator of osteogenesis, initiating the transcriptional program required for osteoblast lineage commitment and early matrix synthesis. Collagen type I (Col-I) represents the primary organic component of bone extracellular matrix and plays a crucial role in providing structural integrity and a scaffold for subsequent mineral deposition. Alkaline phosphatase (ALP) is an early-stage osteogenic marker that contributes to the initiation of mineralization by hydrolyzing phosphate esters, thereby increasing local inorganic phosphate levels essential for calcium phosphate crystal formation. Together, the coordinated upregulation of Runx2, Col-I, and ALP serves as a molecular signature of osteogenic differentiation and bone matrix maturation. The effect of CuO nanoparticles on the expression of osteogenic genes was evaluated after 7 days of culture (Fig. 5). Compared with the control group, cells treated with CuO NPs in osteogenic medium demonstrated a significant upregulation of Runx2, indicating enhanced transcriptional activation driving osteoblast lineage specification. A similar trend was observed for Col-I, where CuO NP treatment led to increased mRNA levels, reflecting augmented extracellular matrix synthesis. Furthermore, ALP expression was significantly elevated, consistent with the initiation of mineralization processes. Collectively, these results confirm that CuO nanoparticles potentiate osteogenic differentiation in C3H10T1/2 cells by promoting the expression of key genes involved in osteoblast commitment, extracellular matrix production, and mineral deposition.

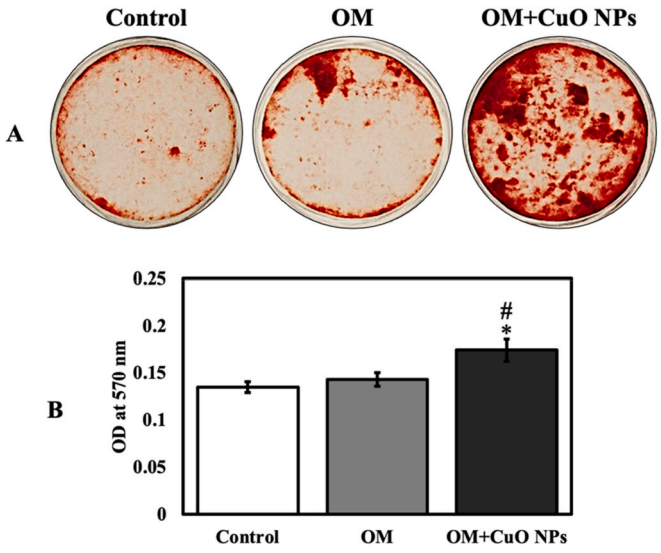

Fig. 4. Effect of CuO nanoparticles on osteogenic differentiation of C3H10T1/2 cells. (A) Representative images of Alizarin Red S staining after 7 days of culture under different conditions: Control (basal medium), OM (osteogenic medium), and OM + CuO NPs (osteogenic medium supplemented with 50 μg/mL CuO nanoparticles). Enhanced mineral deposition is visible in the OM + CuO NP group compared to OM alone and untreated control. (B) Quantitative analysis of Alizarin Red staining following dye elution measured at 570 nm. Data are expressed as mean ± SD from three independent experiments. *$p < 0.05$ compared to control; #$p < 0.05$ compared to OM group.

4. Discussion

This study demonstrates that biogenically synthesized CuO nanoparticles (CuO NPs) using *Alpinia calcarata* extract are structurally pure, cytocompatible up to 50 μg/mL, and capable of potentiating osteogenic differentiation in C3H10T1/2 cells. Our findings highlight the dual advantage of green synthesis and copper's biological role in bone tissue engineering. Plant-mediated nanoparticle synthesis is increasingly favored due to eco-friendly processes and inherent capping by phytochemicals such as flavonoids and phenolics. The FTIR profile of our CuO NPs confirmed the presence of hydroxyl and carbonyl groups, consistent with prior reports showing that plant-derived moieties stabilize CuO NPs and reduce aggregation.[16,17] Similar spectral fingerprints have been reported in biogenic CuO prepared from Corchorus olitorius and Fortunella japonica extracts,[18,19] supporting the reproducibility of this approach. The MTT and FDA data indicated that CuO NPs maintain >80 % viability up to 50 μg/mL, while higher doses decreased survival significantly. This biphasic profile aligns with copper's known biological duality—acting as a cofactor at low doses but causing oxidative stress at excess concentrations. Comparable dose-dependent effects were described in mammalian cells exposed to copper-based biomaterials, with viability preserved below 100 μg/mL but reduced at higher levels.[20,21] Our findings therefore reinforce the need to define safe thresholds before clinical translation. A marked increase in Alizarin Red S staining in the OM + CuO NP group confirmed their role in promoting mineral deposition. Similar outcomes were observed with copper-doped mesoporous bioactive glasses, where Cu release accelerated apatite deposition and enhanced osteoblast function.[16] Karkehabadi et al. (2023) further reported that CuO NPs combined with LED irradiation increased ALP activity and calcium deposition in dental pulp stem cells, highlighting copper's consistent osteoinductive role.[22] Moreover, copper-substituted scaffolds have been shown to enhance osteogenesis–angiogenesis coupling, supporting bone regeneration in vivo.[23] Together, these comparisons suggest that our A. calcarata–derived CuO NPs exert osteo-promotive effects comparable to more complex copper-doped scaffolds. At the gene level, we observed significant upregulation of Runx2, Col-I, and ALP—genes central to osteoblast differentiation. Runx2 is recognized as the master transcriptional regulator of osteogenesis, and its induction drives both early (ALP) and matrix (Col-I) programs.[24] The Col-I increase in our study is consistent with copper's role in collagen matrix assembly, while ALP upregulation reflects initiation of mineralization.[25] Several pathways likely underpin these results. Copper serves as a cofactor for lysyl oxidase (LOX), which

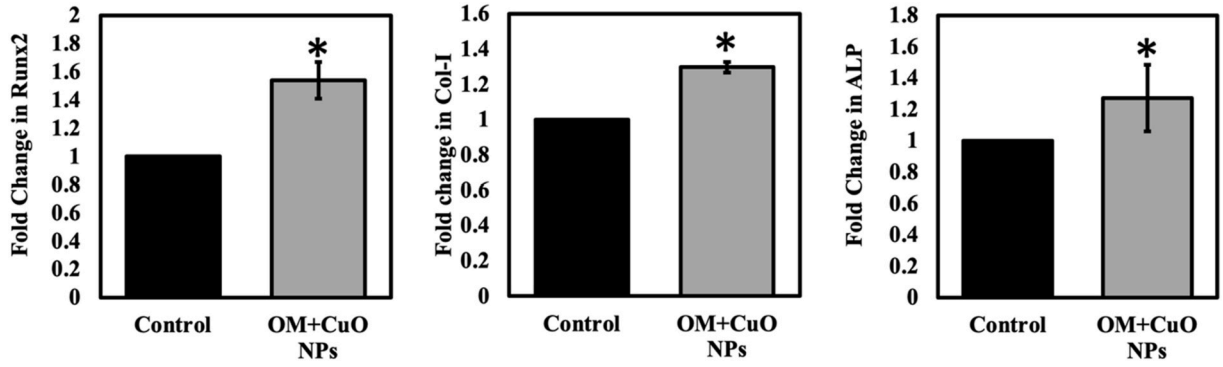

Fig. 5. Effect of CuO nanoparticles on osteogenic gene expression in C3H10T1/2 cells. Relative mRNA expression levels of (A) Runx2, (B) Col-I, and (C) ALP after 7 days of culture in osteogenic medium with CuO NPs (50 μg/mL) compared with control cells. Data are expressed as fold change relative to control (normalized to GAPDH). Values represent mean ± SD from three independent experiments. *$p < 0.05$ compared with control.

catalyzes collagen crosslinking, a prerequisite for mineral deposition.[26] Copper is also a well-established angiogenic factor via HIF-1α and VEGF upregulation, and angiogenesis strongly correlates with osteogenesis.[3] Recent in vivo studies show that copper-containing biomaterials stimulate neovascularization alongside new bone formation,[27] suggesting that the Runx2 and ALP increases seen here may reflect copper's broader role in coupling vascular and osteogenic programs. Compared with scaffold-embedded copper systems, our colloidally delivered CuO NPs achieved similar osteogenic activation in a short 7-day window, underscoring their potential as soluble osteo-boosters or scaffold coatings. Given their phytochemical capping, such NPs may offer improved cytocompatibility and reduced residual toxicity relative to chemically synthesized CuO. This study, however, focused on early differentiation (7 days) and a single working concentration (50 μg/mL). Future work should examine late markers such as osteocalcin and osteopontin, extend culture periods to 14–21 days, and validate protein expression. In vivo models are essential to confirm safety, angiogenesis, and true regenerative potential. Our findings, when compared with existing copper-enabled biomaterials, suggest that green-synthesized CuO NPs can serve as sustainable, multifunctional nanomaterials for bone tissue engineering.

5. Conclusion

In this study, copper oxide nanoparticles were successfully synthesized using *Alpinia calcarata* leaf extract through a simple, eco-friendly biogenic route. The nanoparticles were crystalline, uniformly distributed at the nanoscale, and exhibited surface functionalization by phytochemicals that likely contributed to their stability and biological compatibility. In vitro assays demonstrated that CuO NPs were cytocompatible up to 50 μg/mL and, under osteogenic conditions, significantly enhanced mineral deposition and upregulated key osteogenic markers, including Runx2, Col-I, and ALP. These findings confirm that biogenic CuO NPs can act as effective stimulators of osteoblast differentiation, comparable to more complex copper-based biomaterials, while offering the added advantages of sustainability and reduced synthesis-related toxicity. Overall, A. calcarata–derived CuO NPs represent a promising multifunctional nanomaterial for future applications in bone tissue engineering and regenerative medicine.

Patient's/Guardian's consent

NA.

Ethical clearance

NA.

Source of funding

Nil.

Declaration of competing interest

The authors declare that they have no known competing financial interests or personal relationships that could have appeared to influence the work reported in this paper.

Acknowledgment

Nil.

References

1. Ajithan L, Ganapathy D, Shanmugam R, Dathan PC. Role of nanoparticles and nanocomposites in bone regeneration. *Trends Biomater Artif Organs*. 2024 Jul 1;38 (3).
2. Bosch-Rué E, Díez-Tercero L, Rodríguez-González R, Bosch-Canals BM, Perez RA. Assessing the potential role of copper and cobalt in stimulating angiogenesis for tissue regeneration. *PLoS One*. 2021 Oct 27;16(10), e0259125.
3. Tan Z, Zhou B, Zheng J, et al. Lithium and copper induce the osteogenesis-angiogenesis coupling of bone marrow mesenchymal stem cells via crosstalk between canonical wnt and HIF-1α signaling pathways. *Stem Cell Int*. 2021;2021(1), 6662164.
4. Fiehn LA, Kunisch E, Saur M, et al. A comparative in vitro and in vivo analysis of the impact of copper substitution on the cytocompatibility, osteogenic, and angiogenic properties of a borosilicate bioactive glass. *J Biomed Mater Res*. 2024 Oct;112(10): 1740–1759.
5. Amin F, Fozia, Khattak B, et al. Green synthesis of copper oxide nanoparticles using Aerva javanica leaf extract and their characterization and investigation of in vitro antimicrobial potential and cytotoxic activities. *Evid base Compl Alternat Med*. 2021; 2021(1), 5589703.
6. Saif S, Tahir A, Asim T, Chen Y. Plant mediated green synthesis of CuO nanoparticles: comparison of toxicity of engineered and plant mediated CuO nanoparticles towards Daphnia magna. *Nanomaterials*. 2016 Nov 9;6(11):205.
7. Siddiqi KS, Husen A. Current status of plant metabolite-based fabrication of copper/copper oxide nanoparticles and their applications: a review. *Biomater Res*. 2020 Jun 3;24(1):11.
8. Neiva J, Benzarti Z, Carvalho S, Devesa S. Green synthesis of CuO Nanoparticles—structural, morphological, and dielectric characterization. *Materials*. 2024 Nov 22;17(23):5709.
9. Gebreslassie YT, Gebremeskel FG. Green and cost-effective biofabrication of copper oxide nanoparticles: exploring antimicrobial and anticancer applications. *Biotechnol Rep*. 2024 Mar 1;41, e00828.
10. Rahman MA, Islam MS. Alpinia calcarata roscoe: a potential phytopharmacological source of natural medicine. *Pharmacogn Rev*. 2015 Jan;9(17):55.
11. Chandrakanthan M, Handunnetti SM, Premakumara GS, Kathirgamanathar S. Topical anti-inflammatory activity of essential oils of Alpinia calcarata Rosc., its main constituents, and possible mechanism of action. *Evid base Compl Alternative Med*. 2020;2020(1), 2035671.
12. Komori T. Regulation of skeletal development and maintenance by Runx2 and Sp7. *Int J Mol Sci*. 2024 Sep 20;25(18), 10102.
13. Selvaraj V, Sekaran S, Dhanasekaran A, Warrier S. Type 1 collagen: synthesis, structure and key functions in bone mineralization. *Differentiation*. 2024 Mar 1;136, 100757.

14. Sekaran S, Vimalraj S, Thangavelu L. The physiological and pathological role of tissue nonspecific alkaline phosphatase beyond mineralization. *Biomolecules*. 2021 Oct 21;11(11):1564.
15. Ling Z, Ge X, Jin C, et al. Copper doped bioactive glass promotes matrix vesicles-mediated biomineralization via osteoblast mitophagy and mitochondrial dynamics during bone regeneration. *Bioact Mater*. 2025 Apr 1;46:195–212.
16. Baino F. Copper-doped ordered mesoporous bioactive glass: a promising multifunctional platform for bone tissue engineering. *Bioengineering*. 2020 May 21;7 (2):45.
17. Thirunavukkarasu R, Nandhagopal M, Thirunavukkarasu S, Raji A, Kamath BR, Venkateswaran L. Ecosynthesis of copper and nickel oxide nanoparticles from Aegle marmelos extract: antimicrobial, antioxidant, and hemolytic activity evaluation. *Mater Lett*. 2025 May 7, 138705.
18. Aljedaani RO, Kosa SA, Abdel Salam M. Ecofriendly green synthesis of copper (II) oxide nanoparticles using corchorus olitorus leaves (Molokhaia) extract and their application for the environmental remediation of direct violet dye via advanced oxidation process. *Molecules*. 2022 Dec 20;28(1):16.
19. Akintelu SA, Folorunso AS, Folorunso FA, Oyebamiji AK. Green synthesis of copper oxide nanoparticles for biomedical application and environmental remediation. *Heliyon*. 2020 Jul 1;6(7), e00938.
20. Rajkumar M, Manickam SI, Davis Presely SI, Prabha G, Kirubakaran D, Farahum F, Ali T, Shkir M, Latha S. Synthesis of chitosan/PVA/copper nanocomposite using Anacardium occidentale extract and evaluating its antioxidant, antibacterial, anti-inflammatory and cytotoxic activities. *Sci Rep*. 2025;15(1):3931.
21. Mavil-Guerrero E, Vazquez-Duhalt R, Juarez-Moreno K. Exploring the cytotoxicity mechanisms of copper ions and copper oxide nanoparticles in cells from the excretory system. *Chemosphere*. 2024 Jan 1;347, 140713.
22. Karkehabadi H, Rahmati A, Abbasi R, et al. Effect of copper oxide nanoparticles and light-emitting diode irradiation on the cell viability and osteogenic/odontogenic differentiation of human stem cells from the apical papilla. *BMC Oral Health*. 2023 Apr 28;23(1):249.
23. Dai Q, Li Q, Gao H, et al. 3D printing of Cu-doped bioactive glass composite scaffolds promotes bone regeneration through activating the HIF-1α and TNF-α pathway of hUVECs. *Biomater Sci*. 2021;9(16):5519–5532.
24. Schroeder TM, Jensen ED, Westendorf JJ. Runx2: a master organizer of gene transcription in developing and maturing osteoblasts. *Birth Defects Res Part C Embryo Today - Rev*. 2005 Sep;75(3):213–225.
25. Yuan X, Wang J, Zhu X, et al. Effect of copper on levels of collagen and alkaline phosphatase activity from chondrocytes in newborn piglets in vitro. *Biol Trace Elem Res*. 2011 Dec;144(1):597–605.
26. Rucker RB, Kosonen T, Clegg MS, et al. Copper, lysyl oxidase, and extracellular matrix protein cross-linking. *The American journal of clinical nutrition*. 1998 May 1;67 (5):996S–1002S.
27. Li K, Cao H, Huang H, et al. Advances in copper-containing biomaterials for managing bone-related diseases. *Regen Biomater*. 2025;12. rbaf014.